# Polymer Size Exponents of Branched Dextrans

**J. A. M. Smit,* J. A. P. P. van Dijk, M. G. Mennen,† and M. Daoud‡**

*Gorlaeus Laboratories, Leiden University, P.O. Box 9502, 2300 RA Leiden, The Netherlands, National Institute of Public Health and Environmental Protection, P.O. Box 1, 3720 BA, Bilthoven, The Netherlands, and Laboratoire Leon Brillouin, CEN Saclay, 91191 Gif-sur-Yvette Cedex, France*

*Received December 17, 1991; Revised Manuscript Received March 7, 1992*

ABSTRACT: The exponent $\nu$ in the power law for the radius of gyration, $R \sim N^{\nu}$, with $N$ the total number of chain segments, has been theoretically examined for randomly branched and regular comblike chains. Values of $\nu$ expected in the limits of good solvent and Θ solvent are compared with corresponding experimental values for dextrans in aqueous solutions. In the dilute regime power laws describing the molecular weight dependence of the radius of gyration, mutual diffusion coefficient, second virial coefficient, and the intensity of neutron scattering indicate clearly the branched nature of the molecules. For the osmotic pressure in the semidilute regime, however, a concentration behavior like that for linear chains is seen. The crossover of these properties can be explained by assuming a randomly branched structure involving relatively long branches.

## Introduction

It is well-known that branched polymers are more compact than their linear equivalents having the same number of segments. Usually this property is expressed by the ratio

$$g = \langle R_G^2 \rangle_b / \langle R_G^2 \rangle_l < 1 \tag{1}$$

where $\langle R_G^2 \rangle_b$ and $\langle R_G^2 \rangle_l$ are the mean-square radii of gyration of the branched and linear molecules, respectively. The root-mean-square radius of gyration $\langle R_G^2 \rangle^{1/2}$, which we shall denote in the following simply by $R$, measures the average size of the molecule. For long linear chains $R$ is expected to obey a scaling relationship[1,2]

$$R \sim N^{\nu_l} a \tag{2}$$

with $N$ the total number of statistical segments taken here sufficiently large and with $a$ being the segment length. The value of $\nu_l$ depends on the quality of the solvent, reaching the theoretical value 0.588 in the good solvent limit where the polymer chain is highly swollen.[3] The combination of eqs 1 and 2 yields the formal relationship for a branched polymer

$$R \sim g^{1/2}(N) N^{\nu_l} a \tag{3}$$

Two particular situations may arise in which eq 3 becomes a power law of $R$ in $N$. First, when $g$ is independent of $N$, we recover eq 2. Secondly, when the structure of branching and the solvent quality are such that

$$g \sim N^{-\mu} \tag{4}$$

eq 3 becomes

$$R \sim N^{\nu_l - \mu/2} a \sim N^{\nu} a \tag{5}$$

where $\nu$ is an exponent dependent on the type of branching and the solvent quality and $\mu$ describes the deviation from linear behavior.

In this paper we examine how the branching in dextrans influences the values of the exponents introduced above. The exact structure of branching of these polymers is still not satisfactorily solved. A main problem is the lack of linear analogons, which impedes a direct experimental determination of the $g$ ratios according to eq 1. On the other hand, it must be realized that the $g_0$ ratios, i.e., the corresponding ratios for ideal chains, describe more directly the topology of the branching than the $g$ ratios to which excluded volume interactions may contribute. Estimation of these effects requires information of the structure of branching. Thus in some respect we deal with a vicious circle. For dextrans dissolved in water, however, there is experimental evidence that eqs 4 and 5 are rather well satisfied over rather large ranges of molar masses.[4-6] Also water turns out to be a good solvent ($\nu_l \sim 0.59$) as the second virial coefficient assumes distinct nonzero values and indicates hard-sphere behavior of the chains[7]

$$A_2 \sim R^3/N^2 \sim N^{3\nu-2} a^3 \tag{6}$$

Thus the significant decrease of the observed exponent, i.e., $\nu = \nu_l - \mu/2$ with $\mu \simeq 0.2$, must be ascribed to branching and not to a poor quality of the solvent. Figure 1 shows an elementary fragment of the dextran molecule. Trifunctional branch units are present in an amount of about 5% of the total number of glucose units.[4] This figure has been found rather constant for different fractions obtained as hydrolysates of the native form.[4]

Using trifunctional branch units, we can generate different topologies which may serve as potential structures or at least acceptable models for dextrans. They are shown in Figure 2. In case a the branch units are randomly interconnected by equal subchains. Obviously, there is no backbone. However, some of a backbone becomes perceptible in case b. Here the branch units are distributed over the backbone and the side chains. In case c all branch units are distributed at constant intervals along the backbone, leading to a regular comb structure. We expect that deviations from linear chain behavior gradually increase from c → b → a. In this paper we shall elaborate models a and c. For both topologies the results of random-flight statistics are known.[8,9] Using the Flory approximation,[1,2] we shall estimate the exponents $\mu$ and $\nu$ in which the excluded volume effect has been incorporated. Finally, we shall discuss earlier assessments of branching in dextrans.[4,6,10]

## Theoretical Section

**The Randomly Branched Chain (Model a).** The randomly branched chain considered here contains $n_b$ trifunctional branch units (Figure 2a). This number is related

† National Institute of Public Health and Environmental Protection.

‡ Laboratoire Leon Brillouin.

0024-9297/92/2225-3585$03.00/0 © 1992 American Chemical Society

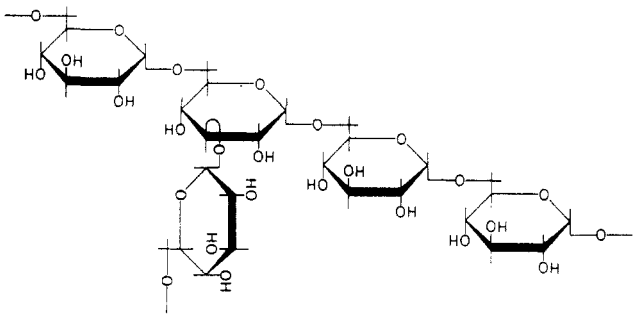

**Figure 1.** Fragmental structure of dextran from *Leuconostoc mesenteroides* B512.

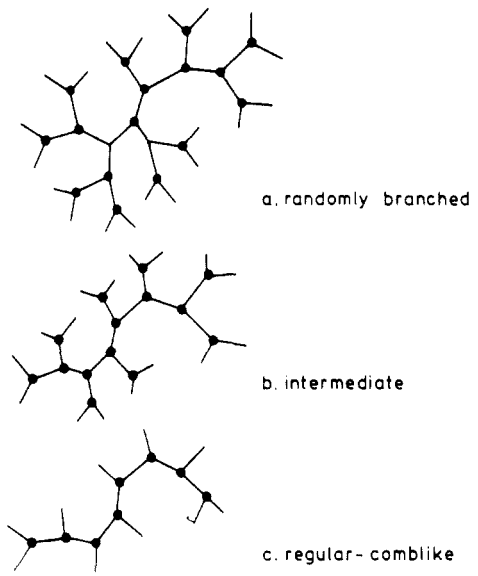


**Figure 2.** Structures for branched chains. In the direction a → b → c the backbone character becomes more pronounced.

to the $N$ segments of the chain and the $n$ segments of the subchains by $n_b = N/(2n) - {}^1/_2$. We shall restrict ourselves to values of $n_b$ larger than 25. Thus $n_b$ will be proportional to $N$ with fixed $n$. Following Zimm and Stockmayer[8] we specify eq 1 to the unperturbed state and define

$$g_0 = R_0^2/({}^1/_6 Na^2) \tag{7}$$

where ${}^1/_6 Na^2$ is just the random-walk result for the equivalent linear chain. Then the $g_0$ factor satisfies the simple expression.

$$g_0 = {}^3/_2 \pi^{1/2}(N/2n)^{-1/2} \qquad n_b > 25 \tag{8}$$

Equation 8 is an approximation of eq 40b in the original paper of Zimm and Stockmayer[8] for $n_b > 25$. Equations 7 and 8 lead to the power law $R_0 \sim N^{1/4}a$. To make this result more realistic we have to take into account the excluded volume interactions between segments. In this context we shall estimate the size of the real chain using the Flory approach for the free energy of a single branched chain in dilute solution. For dimension $d$ in space it reads quite generally[1,2,11,12]

$$F/k_BT = R^2/R_0^2 + vN^2/R^d + wN^3/R^{2d} + \ldots \tag{9}$$

where $k_BT$ has its usual meaning and unimportant constants have been omitted. The first term on the right-hand side of eq 9 describes the elastic contribution to the free energy. It is assumed that all segments are involved in the tendency to bring the molecule back to its Gaussian size. The remaining terms on the right-hand side of eq 9 reflect the opposite tendency of the molecule to swell by excluded volume interactions. The quantities $v$ ($\sim a^d$) and $w$ ($\sim a^{2d}$) stand respectively for the pairwise and triple interactions between segments. Minimization of $F$ with respect to $R$ yields the intermediate result

$$0 = 12R/(g_0 Na^2) - dvN^2/R^{d+1} - 2dwN^3/R^{2d+1} \tag{10}$$

from which $R_0$ has been eliminated by eq 7. In the good-solvent limit $v > 0$ one finds neglecting $w$ and higher order interactions for $d = 3$

$$R \sim N^{3/5} g_0^{1/5} a \qquad (d = 3) \tag{11}$$

Under Θ conditions, defined by $v = 0$, and under the assumption that only triple contacts contribute to eq 10 the latter can be rearranged to

$$R_\Theta \sim N^{1/2} g_0^{1/8} a \qquad (d = 3) \tag{12}$$

Insertion of the expression (8) for $g_0$ into eqs 11 and 12 yields respectively

$$R \sim N^{1/2} a \tag{13}$$

and

$$R_\Theta \sim N^{7/16} a \tag{14}$$

which are the power laws describing the dependence of $R$ on $N$ for randomly branched chains. The corresponding laws for linear chains follow also from eqs 11 and 12 by taking the crossover $g_0 \to 1$. Finally, the exponents $\mu$ and $\mu_\Theta$ in eq 4 are easily evaluated using eqs 5 and 11–14. Values of the exponents $\mu$ and $\nu$ are collected in Table I together with the "unperturbed" values for comparison. The validity of the results needs some comment. Although eqs 11 and 12 have been obtained by a Flory argument involving some kind of a mean field approximation, they proved to be valid below the critical dimension $d_c$ where the chains behave in an ideal manner. In the case of eq 11, $d_c = 4$ for linear chains and $d_c = 8$ for randomly branched chains, whereas correspondingly $d_c = 3$ and $d_c = 6$ for eq 12. The values $\nu = {}^3/_5$ ($d = 3$, $d_c = 4$) and $\nu_\Theta = {}^1/_2$ ($d = d_c = 3$) for linear chains are surprisingly close to the familiar experimental values. The value ${}^3/_5$ is also close to the cited value $\nu = 0.588$.[3] The exponent $\nu = {}^1/_2$ for a randomly branched chain in a good solvent, first derived by Isaacson and Lubensky[11] by the Flory approach, has been confirmed by the solution of an equivalent problem[13] and also by a Monte Carlo calculation.[14] There is still no reliable confirmation of the result $\nu_\Theta = {}^7/_{16}$ obtained first by Daoud and Joanny.[12]

**Table I**
**Theoretical Predictions of Exponents**

| | $\mu_0$ | $\mu_\Theta$ | $\mu$ | $\nu_0$ | $\nu_\Theta$ | $\nu$ |
|---|---|---|---|---|---|---|
| randomly branched chain (model a) | 1 | ${}^1/_8$ | ${}^1/_5$ | ${}^1/_4$ | ${}^7/_{16}$ | ${}^1/_2$ |
| linear or comblike chain (model c) | 0 | 0 | 0 | ${}^1/_2$ | ${}^1/_2$ | ${}^3/_5$ |

**The Regular Comb (Model c).** In the regular comb $f$ branches consisting of $n_1$ segments appear at constant intervals of $n_0$ segments along the backbone (Figure 2c with $n_1 \neq n_0$). The polymer chain contains $N$ segments, $N_0$ of which belong to the backbone. Consequently, $N_0 = fn_0 + n_0$ and $N = (n_0 + n_1)f + n_0$. For $f \gg 1$, $f$ becomes proportional to $N_0$ and with uniform branch length (constant $n_1$) proportional to $N$. The structure of the comb depends also on the ratio $n_1/n_0$, which will be called hereafter $\gamma$. We shall use $f$ and $\gamma$ as descriptive parameters for $g_0$.

Casassa and Berry[9] obtained an expression (cf. eq 20 of ref 9) which in terms of $f$ and $\gamma$ reads

$$g_0 = \left(1 + \frac{f}{f+1}\gamma\right)^{-3}\left[1 + \frac{2f^2}{(f+1)^2}\gamma + \frac{(2f+f^2)}{(f+1)^2}\gamma^2 + \frac{(3f^2-2f)}{(f+1)^3}\gamma^3\right] \quad (15)$$

If the backbone length is much larger than the branch length, i.e., $N_0 \gg n_1$ or $f+1 \gg \gamma$, eq 15 is well approximated by[9]

$$g_0 = \left(1 + \frac{f}{f+1}\gamma\right)^{-1} = \frac{N_0}{N} \quad (16)$$

The ratio $N_0/N$ represents the fraction of linear material in the chain. If $f$ assumes values above $8.33(N_0/N)^{-1}(1 - N_0/N)^{7/3}$, the accuracy of $g_0$ in eq 16 is better than 4% (see p 890 of ref 9 or eq 26 in ref 6). For very long backbones (formally $f \to \infty$) and with $\gamma$ constant, $g_0$ tends to $(1+\gamma)^{-1}$ and becomes independent of $N$.

Equation 16 may be rewritten with eq 7 as

$$R_0^2 = {}^1/_6 N_0 a^2 \qquad (f+1 \gg \gamma) \quad (17)$$

which shows that the unperturbed mean-square radius of gyration behaves as a linear chain of $N_0$ segments in a random walk.

For real regular combs we expect the relationships

$$R \sim (1+\gamma)^{-x} N^{3/5} \qquad (f \to \infty) \quad (18)$$

$$R_\Theta \sim (1+\gamma)^{-x_\Theta} N^{1/2} \qquad (f \to \infty) \quad (19)$$

where we have taken the corresponding $\nu$ exponents of real linear chains. The exponent ${}^3/_5$ is consistent with the linear exponents found by Monte Carlo simulations[15] and renormalization group theory[16] for infinitely long backbones in the good solvent limit. Also the exponent ${}^1/_2$ has been found by Monte Carlo calculations.[17] From the cited calculations[15,17] we estimate, when $f+1 \gg \gamma$, that globally $x \approx {}^3/_{10}$ in eq 18 and $x_\Theta \approx {}^1/_4$ in eq 19, implying that $g \sim (1+\gamma)^{-3/5}$ and $g_\Theta \sim (1+\gamma)^{-1/2}$. Thus in both cases $g > g_0$ for $f \to \infty$. It must be noticed that $g_0$ and $g$ only at large values of $N$ (or $f$) become independent of $N$. Therefore it is clear that long regular combs with constant $\gamma$ show power laws in $N$ (eqs 18 and 19) with the same exponents as linear chains (Table I). Their branched properties, however, become apparent in the values of $g < 1$ when $\gamma > 0$.

**Osmotic Pressure in Semidilute Solutions of Branched Chains.** In the former theoretical sections we discussed single-chain properties which are observed at small values of the polymer concentration. Let us introduce the concentration $c$ expressed as number of segments per unit of volume. We let $c$ increase to some crossover value $c^*$ and consider only the limit where the branched chains are in the highly swollen state. As in the case of linear chains we define $c^*$ by the proportionality $NR^{-3}$.[2] Hence we may write using eq 5

$$c^* \sim N^{(1-3\nu)} a^{-3} \quad (20)$$

At $c^*$, the onset of the semidilute regime, the branched chains are expected to start to overlap. As a result the osmotic pressure $\Pi(c,N)$ becomes independent of $N$. It can be conveniently brought into the form of a power law[18]

$$\Pi/k_B T \sim c/N(c/c^*)^x \quad (21)$$

which is easily shown to be independent of $N$ for $x = 1/(3\nu - 1)$. Using eq 20, we can rewrite eq 21 as

$$\Pi/k_B T \sim c^{3\nu/(3\nu-1)} a^{3/(3\nu-1)} \quad (22)$$

Daoud and Joanny[12] have analyzed the behavior of monodisperse randomly branched chains in semidilute solution. They conclude that in the region $c^* < c < \tilde{c}$ chain overlap is marginal. The crossover concentration $\tilde{c}$ is just the concentration where the segments of the linear subchains overlap. It is defined as

$$\tilde{c} \sim n/(n^{3/5}a)^3 \sim n^{-4/5}a^{-3} \quad (23)$$

It is of interest to compare $\tilde{c}$ with $c^*$, which, using eqs 8 and 11 in this case, is

$$c^* \sim NR^{-3} \sim n^{-3/10}N^{-1/2}a^{-3} \quad (24)$$

Combination of both equations results in

$$\tilde{c} \sim (N/n)^{1/2} c^* \quad (25)$$

The foregoing has particular consequences for the dependence of $\Pi$ on $c$. At $c = c^*$, we have $\Pi/k_B T \sim c^*/N$. In the region $c^* \le c \le \tilde{c}$ we obtain from eqs 21 and 24

$$\Pi/k_b T \sim (c/N)(c/c^*)^2 \sim c^3 a^6 n^{3/5} \qquad (c^* \le c < \tilde{c}) \quad (26)$$

This equation reduces to $\Pi/k_B T \sim \tilde{c}/n$ at $c = \tilde{c}$, which is found by substitution of eq 25 in eq 26. Above $c = \tilde{c}$, given by eq 23, we have analogously to eq 21

$$\Pi/k_B T \sim (c/n)(c/\tilde{c})^x \quad (27)$$

which becomes independent of $n$ for $x = {}^5/_4$

$$\Pi/k_B T \sim (c/n)(c/\tilde{c})^{5/4} \sim c^{9/4}a^{15/4} \qquad (c \ge \tilde{c}) \quad (28)$$

similar to the scaling relationship for linear chains.[18] Thus at $c = \tilde{c}$ there is a crossover from branched-chain to linear-chain behavior and correspondingly the exponent of $c$ in the power law for $\Pi$ changes from 3 to ${}^9/_4$.

**Scaling Relationships Involving the Exponent $\nu$.** As we discussed already the exponent $\nu$ introduced in the power law of $R$ in $N$ (eq 5) appears also as a parameter in the exponents of the corresponding power laws of $A_2$ (eq 6) and $\Pi$ (eq 22). Another example of interest is the structure factor $S(q)$ of an excluded volume chain, where $q$ is the magnitude of the scattering vector. Using a scaling argument,[2] it can be shown to have the general form

$$S(q) \sim N\, f(qR) \sim N\, f(qN^\nu) \quad (29)$$

In the intermediate range $R^{-1} \ll q \ll a^{-1}S(q)$ should be independent of $N$. If, moreover, the function $f(qR)$ is approximated by a power law $(qR)^x$, we get successively

$$S(q) \sim N(qN^\nu)^{-1/\nu} \sim q^{-1/\nu} \quad (30)$$

This expression could be tested in a neutron scattering experiment and the result might indicate a form of self-similarity. Other scaling relationships can be derived from eq 20 for $c^*$ because we have the proportionalities[2]

$$A_2 M \sim [\eta] \sim c^{*-1} \quad (31)$$

where $[\eta]$ denotes the intrinsic viscosity. Finally, one may expect that the diffusion coefficient obtained in a solvent with viscosity $\eta_s$ from quasi-elastic light scattering experiments behaves according to[2]

$$D \sim \left[\frac{k_B T}{\eta_s a}\right] N^{-\nu} \quad (32)$$

as long as the hydrodynamic radius scales like $R$.

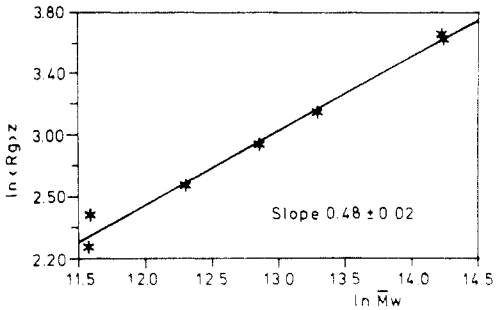


**Figure 3.** GPC–MALLS measurements of the $z$-average radii of gyration (nm) and the weight-average molecular weights (g/mol) for different dextran fractions in 0.1 M $KNO_3$.

## Experimental Section

**Materials.** Dextran samples (Type nRRL-B512) were supplied and kindly donated in part by AB Pharmacia (Uppsala, Sweden). Spread over the whole measuring program about 20 different fractions were used with $\bar{M}_w$ ranging from 10 to 1600 kg mol$^{-1}$ (code numbers T10 to T2000). In addition 6 samples were prepared in the $\bar{M}_w$ range 100–600 kg mol$^{-1}$ by fractionating T2000 and T500 over GPC columns. Characterization data of most of these fractions have been published elsewhere.[19,20] Ratios of $\bar{M}_w/\bar{M}_n$ were found in a range of 1.1 to about 2.5. Thus polydispersity corrections were necessary.

**ELS (Elastic Light Scattering).** Second virial coefficients ($A_2$) were measured in aqueous solutions with or without added salt at 25 °C on a Fica photometer ($\lambda$ = 436 nm) and evaluated from a Zimm plot. The water was purified by a Millipore apparatus. Before the measurement the solutions were filtered through a 0.22-$\mu$m Millipore filter to remove dust particles. Polydispersity corrections for $A_2$ were made assuming hard-sphere interaction between chains[21] and using the chromatograms from GPC for the molecular weight distributions. In addition, Dextran T70 was dissolved in a water/acetone mixture (70/30 vol %), and $A_2$ was measured as a function of the temperature. $T$ = $\Theta$ was estimated as 27.5 °C, where $A_2$ was found to be zero by interpolation.

**QUELS (Quasi-Elastic Light Scattering).** Dynamic light scattering measurements were made with a Malvern photon correlation spectrometer 4300 equipped with an argon laser ($\lambda$ = 519.5 nm) and connected to a Malvern digital correlator (k7023/2). Solutions were prepared as for the ELS measurements. For the $\Theta$ solvent a more open filter was used. The measuring temperature was 25 °C for the usual solutions and 27.5 °C for the water/acetone solvent. The $z$-average diffusion coefficient was evaluated as usual from the decay of the autocorrelation function. Polydispersity correction was made by calculating the molecular weight $M_D$ (see eq 4 of ref 22) corresponding to $D_z$. The exponent $\nu$ was found in an iterative way using the chromatograms obtained by GPC.

**GPC (Gel Permeation Chromatography)–MALLS (Multiangle Laser Light Scattering).** Dextran samples dissolved in 0.1 M $NaNO_3$ aqueous solutions were separated on Type PW TSK columns (G6000–G5000–G3000, Toyo Soda). The instrumentation consisted of a MALLS detector ($\lambda$ = 633 nm), Type Dawn-F (Wyatt Co.), coupled to a Waters 150 C GPC equipped with a RI (refractive index) detector. For eight samples the $z$-average radius of gyration was measured together with the weight-average molecular weight at 25 °C. In addition, both quantities were also evaluated at the peak positions of the RI chromatograms. Along the latter route it is in principle possible to circumvent the polydispersity effect on the molecular weight dependence of the radius of gyration, although the accuracy is poor (see Table III).

**SANS (Small-Angle Neutron Scattering).** SANS measurements were performed in the laboratory "Leon Brillouin", CNRS Saclay, with dextran samples dissolved in pure $D_2O$ and with the following characteristics: T150, $\bar{M}_w$ = 154 kg mol$^{-1}$, $\bar{M}_w/\bar{M}_n$ = 1.79; T70-II-1, $\bar{M}_w$ = 158 kg mol$^{-1}$, $\bar{M}_w/\bar{M}_n$ = 1.17; T2000, $\bar{M}_w$ = 1526 kg mol$^{-1}$, $\bar{M}_w/\bar{M}_n$ > 3. The concentrations of the solutions were chosen at and below $c^*$ (Table II). Spectra of $S(q)$ vs $q$ were obtained and corrected for the contribution of the empty cell and the effect of incoherent scattering. The latter was estimated from the plateau observed in the spectrum of $S(q)$ vs $q$ and the calculated concentration of $H$ of each sample. A perfect linear relationship was found between the plateaus and $C_H$.

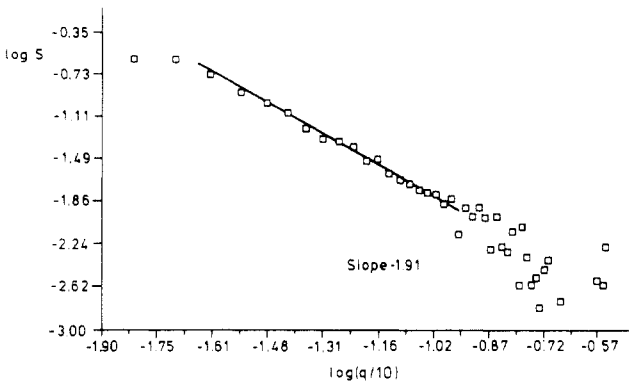


**Figure 4.** SANS measurements from a solution ($c$ = $^1/_2c^*$) of the narrow dextran fraction T70-II-1 in $D_2O$ showing power law behavior in the intermediate range of $q$ values ($S$ dimensionless and $q$ in (nm)$^{-1}$).

**Table II**
**Experimental Values of $1/\nu$ Calculated According to Relationship 30**

| sample | concn | $1/\nu$ | $q$ range [(nm)$^{-1}$] |
|---|---|---|---|
| T150 | $c^*$ | 2.10 | 0.35–1.3 |
| T150 | $^1/_2c^*$ | 1.91 | 0.30–1.3 |
| T150 | $^1/_{10}c^*$ | 1.94 | 0.25–0.8 |
| T70–II–1 | $c^*$ | 2.04 | 0.30–1.3 |
| T70–II–1 | $^1/_2c^*$ | 1.91 | 0.25–1.1 |
| T70–II–1 | $^1/_{10}c^*$ | 1.91 | 0.09–0.04 |
| T2000 | $^1/_2c^*$ | 1.93 | 0.09–0.03 |

$R$(T150;T70-II-1) ≃ 12.8 nm
$R$(T2000) ≃ 36.4 nm
persistence length[6] ≃ 2.5 nm

**Osmometry.** Osmotic pressures were measured in water at 25 °C with a Model 230 Wescan osmometer equipped with a RC 51 cellulose membrane supplied by Schleicher & Schuell (Dassel, Germany). The principle and procedure of measuring have been reported in detail.[23] For the rather large osmotic pressures in the semidilute regime it was sometimes not possible to obtain them with the solvent as reference. In that case the osmotic pressure difference between two solutions was measured. The desired osmotic pressure could then be stepwise calculated.

## Results and Discussion

In Figure 3 the $z$-average radius of gyration is seen to obey a power law $\sim \bar{M}_w^{0.48}$ over a rather wide range of molecular weights. The exponent is larger than the values found in water, i.e., 0.43[4] and 0.45,[24] partly because added salt improves the solvent quality. Another power law is tested in Figure 4, where, according to the predictions of eq 30, a log–log plot of the scattering intensity and the value of the scattering sector yields a straight line in the intermediate range of $q$ values. Values of the exponent $1/\nu$ are compiled in Table II. They are found to be clustered around 2 independent of the concentration, polydispersity, and the molecular weights of the dextran samples. The above findings support strongly that self-similar structures are generated during the bacteriological synthesis of dextran.

In Table III values of $\nu$ are collected which, unless indicated, have been corrected for polydispersity. They result from experimentally observed power laws for $R$, $A_2$, $S(q)$, and $D$ in conformity to eqs 5, 6, 30, and 32. The value $\nu$ = 0.46 obtained by QELS in water lies just between

Table III
Experimental Values of the Exponent $\nu$

| method | measd quantity | solvent | $T$ (°C) | $\bar{M}_w$ (kg/mol) | no. of points | $\nu$ |
|---|---|---|---|---|---|---|
| GPC-MALLS | $R$ | 0.1 M $NaNO_3$ | 25 | 100–1600 | 8 | 0.47 ± 0.06 |
| | | | | | 8 | 0.48 ± 0.02[a] |
| Rayleigh[b] interferometry | $D$ | water | 30 | 10–110 | 8 | 0.48 |
| QELS[c] | $D$ | water | 25 | 20–1600 | 4 | 0.46 ± 0.00 |
| QELS | $D$ | 1 M NaCl | 25 | 10–1600 | 9 | 0.49 ± 0.01 |
| QELS[c] | $D$ | 1 M NaCl | 25 | 10–1600 | 6 | 0.50 ± 0.01 |
| ELS[c] | $A_2$ | water | 25 | 10–1600 | 8 | 0.46 ± 0.01 |
| ELS[c] | $A_2$ | 1 M NaCl | 25 | 40–650 | 3 | 0.47 ± 0.01 |
| SANS | $-1/\nu$ | $D_2O$ | 25 | 150, 1600 | 7 | 0.51 ± 0.02 |
| QELS | $D$ | water/acetone (70%/30%) | 27.5 | 40–650 | 8 | 0.40 ± 0.03 |
| viscosity | $[\eta]$ | 0.1 M $KNO_3$ | 25 | 10–550 | 7 | 0.48[a] |

[a] Without correction for polydispersity. [b] Reference 26. [c] Reference 27.

the literature data $\nu = 0.45$[22] and $\nu = 0.485$.[25] Again it is seen that adding of salt to the solvent water causes a larger value of the exponent $\nu$. The exponents $\nu$ determined from $A_2$ agree with those resulting from $R$, proving that eq 6 is consistent with eq 5. It means that in the range of values observed for $\nu$ the solvent quality is good and the chains behave as hard spheres. On the contrary, for the Θ solvent the significantly small value $\nu = 0.40$ is found. Thus the global picture emerging in Table III is that the solvent quality varies from $\nu_\Theta \approx 0.4$ (poor or Θ solvent) to $\nu_\Theta \approx 0.5$ (good solvent). These limiting values of $\nu$ agree strikingly with those predicted by the randomly branched structure (model a) and shown in Table I. So we are led to the conclusion that probably some type of random branching in the dextran molecules is responsible for the observed behavior of the exponents $\nu$, which cannot be explained by the regular comb model (model c with $n_1 \neq n_0$).

Other types of regular combs have been proposed as possible structure models for dextrans.[6,10] Here the $g_0$ ratio is also considered to obey eq 16, but the rather artificial assumption has been made that $\gamma$ depends on $N$, which, in turn, makes $g_0$ strongly dependent on $N$. More precisely, it is assumed that $n_1 + n_0$ remains constant and $n_1$ increases strongly with increasing $N$. This model does not enable us to explain the observed self-similarity of the dextran chains. Moreover, it predicts a too weak dependence of $g$ on $N$, i.e., $\mu \approx 0.1$.[24] In this respect it is interesting to note that Granath has proposed $\mu \sim 0.19$,[5,6] which is close to the value $^1/_5$ for randomly branched chains (Table I).

So far we have seen that the branched properties of dextrans are clearly visible in the dilute concentration region. It seems worthwhile to inspect also the behavior of the chains in semidilute regimes. In Figure 5 the osmotic pressure is seen to follow a power law in the concentration as predicted by eq 22. Note that the curves of the different dextran fractions, including the data obtained by Vink,[28] tend to a single straight line. Using only our own data, the slope of this line, being $3\nu/(3\nu - 1)$, turns out to be 2.20 ± 0.05. For both T250 and T2000, for which the data are spread over a large concentration range, the same value $3\nu/(3\nu - 1) = 2.22 \pm 0.03$ is found. The observed behavior of Π agrees almost completely with the theoretical results $\Pi \sim c^{9/4}$ expected for linear chains under good-solvent conditions[29] (eq 22 with $\nu = {}^3/_5$). There is also a good agreement with the empirical relation $\Pi \sim c^{2.22\pm0.12}$ found for a great variety of polymer–good solvent systems.[30] The above findings have interesting consequences. Apparently, we observe a regime described by eq 28 which predicts the scaling behavior in Figure 5 for the linear subchains. On the other hand, we expect in the more dilute regime the branching of the molecules. In this respect it is useful to

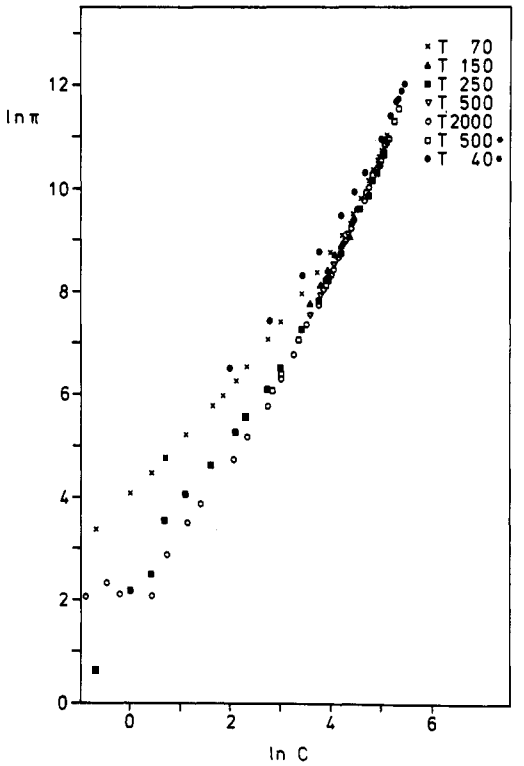


**Figure 5.** Osmotic measurements of aqueous solutions of dextrans showing the power law $\Pi \sim c^{2.20\pm0.05}$ in the semidilute region, with Π in $N$ m$^{-2}$ and $c$ in kg m$^{-3}$. The asterisk refers to measurements of Vink.[28]

try the relationship $\Pi N/c = f(c/c^*)$ or rather $\Pi N/c = f(c[\eta])$. A plot on this basis is shown in Figure 6. Obviously, we have to take care of the polydispersity of the samples ($\bar{M}_n$ and $[\eta]$). The points in Figure 6 are seen to form a single master curve below $c[\eta] \sim 1.5$. If we calculate $c^*$ for the different dextran fractions from $\bar{M}_w$ and $R$, we find the relationship $c^*[\eta] = 1.4 \pm 0.1$. It implies that in the dilute regime $\nu$ is about $^1/_5$ for $c^*$ in eq 20 (see also Table III and eq 31). Thus the osmotic pressure shows rather universally the branching properties of whole molecules in the dilute regime, if it is scaled in the appropriate way. For Dextrans T250 and T2000 the crossover concentrations $\tilde{c}$ were estimated respectively at 80 and 70 kg m$^{-3}$, which corresponds respectively to values of $\tilde{c}[\eta]$ of 3.5 and 4.8. These findings are in accordance with the prediction of eq 25 that $\tilde{c}$ must be larger than $c^*$. However, the difference between both concentrations is not extremely large, and we do not observe the typical regime between them which is described by eq 16. This is probably caused by the fact that randomly distributed long branches are present in dextran molecules as was

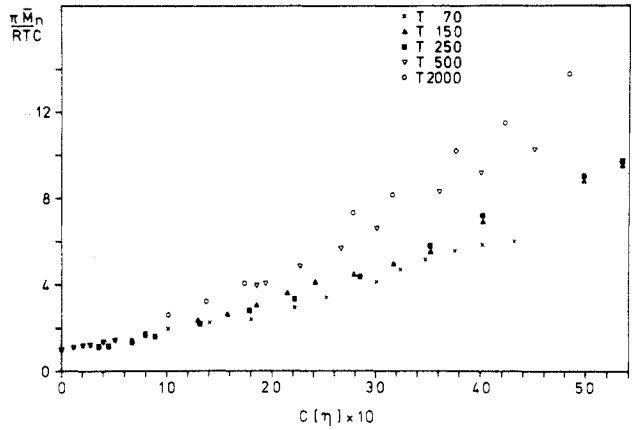


**Figure 6.** Osmotic measurements of aqueous solutions of dextrans showing scaling behavior in the dilute regime. The variables are dimensionless, with $\bar{M}_n$ in kg mol$^{-1}$, RT in J mol$^{-1}$, $[\eta]$ in m$^3$ kg$^{-1}$, and $\Pi$ and $c$ as in Figure 5.

suggested a long time ago.[4,31] Finally, we remark that here we have an example where going from the dilute to the semidilute regime a crossover is observed from branch properties to quasi-linear properties of macromolecules. This crossover was just predicted by Daoud and Joanny[12] for monodisperse randomly branched chains.

## Conclusions

The experimentally determined exponent $\nu$ of dilute aqueous solutions of dextrans lies in a range between 0.4 (poor-solvent limit) and 0.5 (good-solvent limit). These findings are close to the theoretical estimations $\nu_\Theta = {}^7/_{16}$ and $\nu = {}^1/_2$ following from the Flory approximation applied to a single randomly branched chain in dilute solution. Although dextran cannot be considered as a real fractal, there is evidence for the presence of randomly distributed branches in the molecule. The observed large deviation from linear behavior cannot be explained by adopting a simple comblike structure. Useful additional information was obtained from osmotic measurements in the semidilute regime. Only linear parts of the molecule are seen, indicating that the subchains are rather long. Moreover, the exponent $\nu$ in that case turns out to be about ${}^3/_5$, which means that water is a good solvent for dextran.

**Acknowledgment.** We are grateful to J. Teixeria for experimental assistance supplied during the SANS measurements and to L. Zaat and J. Vennix for performing some experiments.

## References and Notes

(1) Flory, P. J. *Principles of Polymer Chemistry*; Cornell University Press: Ithaca, NY, 1953.
(2) de Gennes, P.-G. *Scaling Concepts in Polymer Physics*; Cornell University Press: Ithaca, NY, 1979.
(3) Le Guillou, J. C.; Zinn-Justin, J. *J. Phys. (Les Ulis, Fr.)* **1989**, *50*, 1365.
(4) Senti, F. R.; Helman, N. N.; Ludwig, N. H.; Babcock, G. E.; Tobin, R.; Glass, C. A.; Lamberts, B. L. *J. Polym. Sci.* **1955**, *17*, 527.
(5) Granath, K. A. *J. Colloid Sci.* **1958**, *13*, 308.
(6) Garg, S. K.; Stivala, S. S. *J. Polym. Sci., Polym. Phys. Ed.* **1978**, *16*, 1419.
(7) This property will be discussed later in the Results and Discussion.
(8) Zimm, B. H.; Stockmayer, W. H. *J. Chem. Phys.* **1949**, *17*, 1301.
(9) Casassa, E. F.; Berry, G. C. *J. Polym. Sci., Part A-2* **1966**, *4*, 881.
(10) Wales, M.; Marshall, P. A.; Weisberg, S. G. *J. Polym. Sci.* **1953**, *10*, 229.
(11) Isaacson, J.; Lubensky, T. C. *J. Phys. (Paris), Lett.* **1980**, *4*, 471.
(12) Daoud, M.; Joanny, J. F. *J. Phys. (Paris)* **1981**, *42*, 1359.
(13) Parisi, G.; Sourlas, N. *Phys. Rev. Lett.* **1981**, *46*, 891.
(14) Glaus, U. *J. Phys. A: Math. Gen.* **1985**, *8*, L609.
(15) Lipson, J. E. G. *Macromolecules* **1991**, *24*, 1333.
(16) Vlahos, C. H.; Kosmas, M. K. *J. Phys. A: Math. Gen.* **1987**, *20*, 1471.
(17) McCrackin, F. L.; Mazur, J. *Macromolecules* **1981**, *14*, 1214.
(18) Daoud, M.; Cotton, J. P.; Farnoux, B.; Jannink, G.; Sarma, G.; Benoit, H.; Duplessix, R.; Picot, C.; de Gennes, P.-G. *Macromolecules* **1975**, *8*, 804.
(19) van Dijk, J. A. P. P.; Varkevisser, F. A.; Smit, J. A. M. *J. Polym. Sci.* **1987**, *25*, 149.
(20) Eggink, G.; van Dijk, J. A. P. P.; Smit, J. A. M. *Polym. Bull.* **1987**, *17*, 531.
(21) See section 27d(ii) in: Yamakawa, H. *Modern Theory of Polymer Solutions*; Harper & Row: New York, 1971. See eqs 11b, 13, and 20 in: Mennen, M. G.; Smit, J. A. M. *Polym. Bull.* **1990**, *23*, 67.
(22) Sellen, D. B. *Polymer* **1975**, *16*, 561.
(23) Mennen, M. G. Thesis, Leiden, 1989.
(24) This value has been calculated from experimental data reported in ref 6.
(25) Snabre, P.; Grossmann, G. H.; Mills, P. *Colloid Polym. Sci.* **1985**, *263*, 478.
(26) Soeteman, A. A. Thesis, Leiden, 1982.
(27) Vogelsang, H. W. J., internal report, 1985.
(28) Vink, H. *Eur. Polym. J.* **1971**, *7*, 1411.
(29) des Cloizeaux, J. *J. Phys. (Paris)* **1975**, *36*, 281.
(30) Roots, J.; Nyström, B. *Polymer* **1979**, *20*, 148.
(31) Antonini, E.; Belleli, L.; Bruzzesi, M. R.; Caputo, A.; Chiancone, E.; Rossi-Fanell, A. *Biopolymers* **1964**, *2*, 27.

**Registry No.** Dextran, 9004-54-0; neutron, 12586-31-1.